ACS APPLIED MATERIALS & INTERFACES

Research Article

www.acsami.org

Effective Immobilization of BMP-2 Mediated by Polydopamine Coating on Biodegradable Nanofibers for Enhanced in Vivo Bone Formation

Hyeong-jin Cho,[†,‡] Sajeesh Kumar Madhurakkat Perikamana,[†,‡,#] Ji-hye Lee,[‡] Jinkyu Lee,[‡,#] Kyung-Mi Lee,[§] Choongsoo S. Shin,*[,⊥] and Heungsoo Shin*[,‡,#]

[‡]Department of Bioengineering, Institute for Bioengineering and Biopharmaceutical Research, Hanyang University, Seoul 133-791, Republic of Korea

[§]Global Research Laboratory, Department of Biochemistry and Molecular Biology, Korea University College of Medicine, Seoul 136-713, Korea

[⊥]Department of Mechanical Engineering, Sogang University, 1 Shinsu-dong, Mapo-gu, Seoul 121-742, Korea

[#]BK21 Plus Future Biopharmaceutical Human Resources Training and Research Team

ABSTRACT: Although bone morphogenic proteins (BMPs) have been widely used for bone regeneration, the ideal delivery system with optimized dose and minimized side effects is still active area of research. In this study, we developed bone morphogenetic protein-2(BMP-2) immobilized poly(L-lactide) (PLLA) nanofibers inspired by polydopamine, which could be ultimately used as membranes for guided bone regeneration, and investigated their effect on guidance of in vitro cell behavior and in vivo bone formation. Surface chemical analysis of the nanofibers confirmed successful immobilization of BMP-2 mediated by polydopamine, and about 90% of BMP-2 was stably retained on the nanofiber surface for at least 28 days. The alkaline phosphatase activity and calcium mineralization of human mesenchymal stem cells (hMSCs) after 14 days of in vitro culture was significantly enhanced on nanofibers immobilized with BMP-2. More importantly, BMP-2 at a relatively small dose was highly active following implantation to the critical-sized defect in the cranium of mice; radiographic analysis demonstrated that 77.8 ± 11.7% of newly formed bone was filled within the defect for a BMP-2-immobilized groups at the concentration of 124 ± 9 ng/cm^2, as compared to 5.9 ± 1.0 and 34.1 ± 5.5% recovery, for a defect-only and a polydopamine-only group, respectively. Scanning and transmission electron microscopy of samples from the BMP-2 immobilized group showed fibroblasts and osteoblasts with nanofiber strands in the middle of regenerated bone tissue, revealing the importance of interaction between implanted nanofibers and the neighboring extracellular environment. Taken together, our data support that the presentation of BMP-2 on the surface of nanofibers as immobilized by utilizing polydopamine chemistry may be an effective method to direct bone growth at relatively low local concentration.

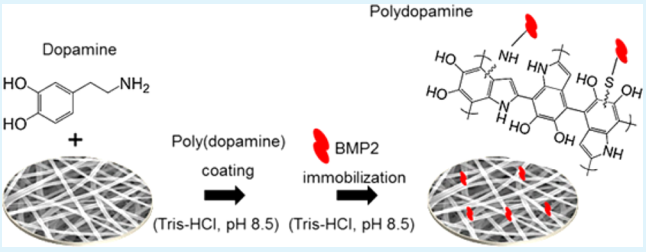

KEYWORDS: *guided bone regeneration, bone morphogenic proteins, nanofibers, electrospinning, osteogenic differentiation, polydopamine*

1. INTRODUCTION

In most clinical cases, bone tissue can be regenerated through its well-known self-healing process. However, self-healing is limited in critical sized defects such as traumatic injury and bone tumor resection. To overcome these clinical conditions, guided bone regeneration has been introduced using a membrane that has suitable pore sizes to prevent undesired tissue infiltration and to direct the new bone formation.[1] Electrospinning is a promising technique to fabricate these membranes and regulating the spinning parameters can generate a range of pore sizes.[2] However, despite excellent characteristics such as mechanical properties and tunable biodegradability, most electrospun fibers of synthetic polymers have shown low cell affinity and insufficient interactions with native bone, mainly because of high hydrophobicity and lack of biofunctional moieties. Many solutions have been proposed to address these problems. For example, coating electrospun poly(ε-caprolactone) (PCL) fibers with gelatin and calcium phosphate enhanced osteogenic differentiation of bone-forming cells.[3,4] Nanohydroxyapatite-coated, plasma-treated electrospun poly(L-lactide) (PLLA) fibers increased osteogenic differentiation of human cord blood-derived somatic stem cells and induced ectopic bone formation.[5] However, these methods resulted in fibers with limited capacity for in vivo bone formation, possibly because of a lack of osteoinductive signals.

Bone morphogenic proteins (BMPs) have been used as strong osteoinductive factors for bone tissue regeneration. Examples of effective targeting of BMPs include the physical

Received: March 8, 2014
Accepted: June 19, 2014
Published: June 19, 2014

adsorption of BMP-2 onto porous scaffolds, the incorporation of BMP-7 into core−shell-type nanoparticles, and the blending of BMP-2 with biodegradable gelatin hydrogels.[6−8] However, challenges to delivery of BMPs in soluble form include denaturation and dosage control. BMPs have also been immobilized onto scaffolds that can continuously and stably induce bone formation.[9] For example, porous collagen scaffolds conjugated with BMP-2 induced osteogenic differentiation of rat bone mesenchymal stem cells and ectopic bone formation in rats. Electrospun poly(dioxanone) membranes conjugated with BMP-2 enhanced alkaline phosphatase (ALP) activity and osteogenic gene expression of MC3T3-E mouse osteoblasts.[6,7] Despite these promising results in previous studies, there are several issues in immobilization of BMP on the surface of biomaterials; biological activity may be impaired by the conformational changes of proteins, and the stability of BMP may also be affected by chemical structure of surface, and organic solvents used during multistep chemical conjugation processes. Moreover, the concentration of immobilized BMP versus as a soluble form, needed for effective bone, is to be fully characterized.

Recently, it was reported that catechol and amine groups within dopamine are responsible for its polymerization in slightly basic solutions to form polydopamine layers on a variety of materials.[10] In addition, polydopamine coating allow the formation of ad-layers of proteins or peptides by chemical conjugation via imine formation or Michael addition.[11,12] For instance, polydopamine-coated stainless steel was used to immobilize vascular endothelial growth factor to control proliferation of endothelial cells and prevent platelet adhesion.[13] Arg-Gly-Asp (RGD) was bound to polydopamine-coated poly(methyl methacrylate) and enhanced in vivo tissue adhesion and host tissue integration.[14] We also reported the immobilization of growth factors or peptides on electrospun fibers prepared from poly(α-hydroxy) ester polymers using polydopamine chemistry.[15−17] However, the majority of previous studies have been limited to in vitro studies and the efficacy of polydopamine coating on presentation of BMP-2 in regulation of in vivo bone formation has never been reported yet.

In this study, we (1) tested polydopamine-coating conditions for effective immobilization and the measurable surface concentration range of BMP-2, (2) investigated how BMP-2 surface concentration affected in vitro adhesion, proliferation and osteogenic differentiation of hMSCs, and (3) examined the concentration-dependent efficacy of bone formation over two months using fibers with immobilized BMP-2 in a mouse calvarial critical size defect model.

2. EXPERIMENTAL SECTION

2.1. Materials and Methods. PLLA with 5.7−8.5 dL/g inherent viscosity was from Evonik (Resomer L214S, Essen, Germany), 1,1,1,3,3,3-Hexafluoro-2-propanol (HFIP) was from Wako (Osaka, Japan), and Tris-HCl was from Alfa Aesar (Heysham, UK). Phosphate buffered saline (PBS), fetal bovine serum (FBS), trypsin-ethylenediaminetetraacetic acid (TE) and penicillin-streptomycin (PS) were from Wisent (Montreal, QC, Canada). Dulbecco's modified eagle medium with low glucose (DMEM) was from Gibco BRL (Rockville, MD, USA). Hoechst 33258 was from Molecular Probes (Eugene, OR, USA), and rhodamine-phalloidin was from Invitrogen Corp. (Carlsbad, CA, USA). Distilled water was produced by an Elix advantage system (Millipore, MA, USA). Dopamine hydrochloride, alizarin red S, and all other reagents were from Sigma-Aldrich (St. Louis, MO, USA). BMP-2 and BMP-2 Quantikine immunoassay kits were from R&D Systems (Minneapolis, MN, USA).

2.2. Preparation of PLLA Nanofibers and Immobilization of BMP-2. PLLA electrospun fibers were fabricated by dissolving PLLA in HFIP with stirring for 3 days. The resulting polymer solution was ejected at 2 mL/h through a 23G blunt-end needle using a syringe pump onto an aluminum foil-covered rotating collector (13kV), 30 cm from the needle. Rotation speed was 200 rpm. Electrospun fibers were dried at room temperature for 1 day, then hydrated with ethanol, and then distilled water. Fibers were immersed in dopamine hydrochloride solution (2 mg/mL, 10 mM Tris-HCL buffer, and pH 8.5) and stirred at 50 rpm for 4 h on an orbital shaker. Samples were thoroughly rinsed and stirred in distilled water overnight. Polydopamine-coated PLLA nanofibers were immersed in BMP-2 solution (250, 500 ng/mL, 10 mM Tris-HCl buffer, pH 8.5) and incubated at 37 °C overnight.

2.3. Characterization of Nanofibers with Immobilized BMP-2. The surface morphology of electrospun nanofibers was examined by field-emission scanning electron microscopy (FE-SEM) (Nova nano SEM 450, FEI, USA). Surface roughness was measured with an atomic force microscope (AFM) (TT-AFM, AFM workshop, CA, USA). Surface atomic composition was analyzed by X-ray photoelectron spectroscopy (XPS) (Theta Probe Base System, Thermo Fisher Scientific, MA, USA) using XPS peak-fitting software (Thermo VG Scientific, MA, USA). Polydopamine on PLLA fibers was quantified using a modified microbicinchoninic acid BCA assay.[18] Polydopamine-coated nanofibers of 1 cm diameter were treated with 300 μL micro-BCA working solution (Pierce, Rockford,IL, USA) and incubated for 2 h at 37 °C. Absorbance was measured at 562 nm using a spectrometer (SpectraMAX M2e. Molecular Device, Sunnyvale, CA, USA). To measure fiber diameter, we took four representative images from each group and diameters measured 30 strands from each image using Nikon imaging software (NIS-Elements AR 3.00, Nikon, Japan).

2.4. Quantification of Immobilized BMP-2. Immobilized amount and long-term release kinetics of BMP-2 was indirectly measured by enzyme-linked immunosorbent assay (ELISA). The nanofibers were treated with 500 μL of BMP-2 solution and incubated overnight at 37 °C. After overnight incubation, BMP-2 in the supernatant was measured with an ELISA kit. Amount of BMP-2 in 500 μL of original solution (which are not treated with nanofibers) was also measured using ELISA and amount of immobilized BMP-2 on nanofibers was calculated as a difference in values of original solutions and in the supernatant solutions. For the long-term release analysis of BMP-2, supernatants were completely collected and freshened with PBS at day 1, 3, 5, 7, 14, 21, and 28. Supernatants from each day were stored at −70 °C until the day of ELISA experiment. All the ELISA experiments were performed according to the manufacturès protocol, and sample absorbance was measured using a spectrophotometer at 450 nm with 540 nm used for λ correction.

2.5. Culturing hMSCs. For in vitro studies, polydopamine-coated nanofibers were punched into circles of 1.91 cm^2 and placed into 24-well culture plates to completely cover the bottoms of the wells. Fibers were sterilized with 70% EtOH, UV light exposure, and then washed several times with PBS. Sterilized nanofibers were further immobilized with BMP-2 by immersing in a solution containing BMP-2 (250, 500 ng/mL, 10 mM Tris-HCl buffer, pH 8.5) followed by overnight incubation at 37 °C. hMSCs from Cambrex Inc. (Charles City, IA, USA) were cultured as monolayers in low-glucose DMEM with 10% FBS and 1% PS at 37 °C, 95% air, 5% CO^2, in a humidified environment. Media was refreshed every 2−3 days. To examine cell behavior on fibers, hMSCs were enzymatically removed from culture flasks using 0.125% trypsin-EDTA and seeded onto fibers at 1×10^4 cells/cm^2 for immunofluorescence and 2×10^4 cells/cm^2 for other experiments. After 12 h, medium was replaced with osteogenic differentiation media with 10% FBS, 1% PS, 50 μg/mL ascorbic acid, 0.01 M glycerol-2-phosphate, and 10−7 M dexamethasone in low-glucose DMEM. Osteogenic differentiation medium was changed every 2−3 days.

2.6. Immunofluorescence Staining. At 1, 7, and 14 days of culture, supernatants were removed and fibers cultured with hMSCs

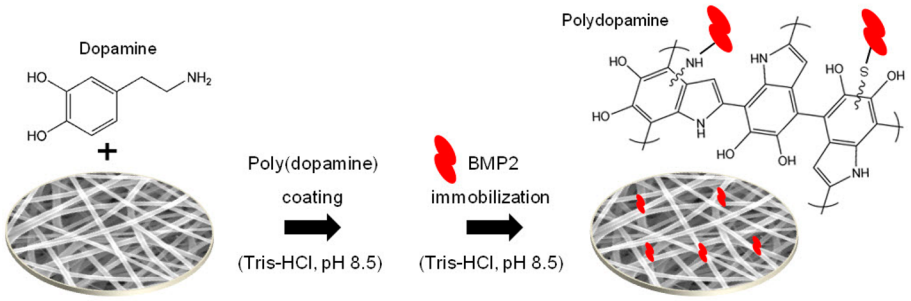

Figure 1. Schematic diagram showing the polydopamine-mediated preparation of electrospun nanofibers with immobilized BMP-2.

were washed twice with PBS and fixed with 4% paraformaldehyde. Fixed samples were permeabilized with cytoskeleton buffer (pH 6.8, 50 mM NaCl, 150 mM sucrose, 3 mM $MgCl_2$, 50 mM Trizma-base, 0.5% Triton X-100) at 4 °C for 20 min followed by incubation with blocking buffer (5% FBS, 0.1% Tween-20 in PBS) for 1 h at 37 °C. Samples were stained for cell nuclei and F-actin using Hoechst 33258 (1:10000) and rhodamine-phalloidin (1:200) in blocking buffer for 1 h at 37 °C. After washing with PBS, samples were mounted with mounting medium (Vectashield, Vector Laboratory, UK), and observed with a confocal microscope (LSM 5 Exciter, Carl Zeiss, Germany).

2.7. SEM of hMSCs on Fibers. Cell adhesion and proliferation of hMSCs on nanofibers was examined using FE-SEM. Samples were treated with glutaraldehyde (1% in PBS) for 30 min followed by 3 h in 4% formaldehyde and graded dehydration in EtOH 30−100%. To ensure complete dryness, we treated samples with hexamethyldisilazane for 15 min. Dried samples were gold coated using a sputter coater (BAL-TEC/SCD 005, BAL-TEC AG, Balzers, Liechtenstein) for 5 min and observed at an acceleration of 5 kV.

2.8. ALP Activity and DNA Assays. ALP activity assays determined the amount of ALP secreted by cells on nanofibers. After 10 days of culturing, nanofibers containing hMSCs were treated with RIPA lysis buffer (150 mM Trizma-base, 150 nM NaCl, 1% sodium deoxycholate, 0.1% SDS, and 1% Triton X-100 in distilled water). Samples were finely chopped with scissors and centrifuged at 13 000 × g for 10 min. Supernatants (10 μL) were treated with 200 μL p-nitrophenyl phosphate (Sigma, St. Louis, MO, USA) at 37 °C for 30 min. Reactions were stopped with 50 μL 3N NaOH and optical density was determined with a spectrophotometer at 405 nm. The same samples were used for DNA assays with Quant-iT PicoGreen dsDNA assay kits (Invitrogen, Carlsbad, CA, USA) according to the manufacturer's procedure. Fluorescence was measured at excitation 480 nm and emission 520 nm using a fluorescence microplate reader (SpectraMAX M2e. Molecular Device). ALP activity was normalized to DNA content.

2.9. Calcium Assay. After 14 days of culture, calcium assays and alizarin red S staining were used to measure calcium deposition. Mineralized calcium deposited by hMSCs on nanofibers was dissolved in 0.6 N HCl. Samples were finely chopped with scissors and incubated at 37 °C overnight. After centrifugation, the amount of deposited calcium in supernatants was quantified using QuantiChrom Calcium Assay kits (Bioassay Systems, Hayward, CA, USA) according to the manufacturer's instructions. Deposited calcium was estimated using absorbance at 570−650 nm measured with a spectrophotometer.

2.10. Mouse Calvarial Defect Model. The effect of BMP-2 immobilized on nanofibers on *in vivo* guided bone regeneration (GBR) was examined using 6-week-old ICR mice (Narabiothec, Seoul, Korea). Animal studies were approved by Institutional Animal Care and Use Committee (IACUC) at Hanyang University (HY-IACUC-12−079) and experiments were performed under IACUC guidelines. Mice were anesthetized with Zoletil (60 mg/kg) and xylazine (20 mg/kg). Scalp hair was shaved and the incision area was sterilized with 70% EtOH. After skin incision, two of 4 mm critical-sized defects were created on both sides of the cranium using a 4 mm-diameter surgical trephine bur. Sterilized nanofibers were implanted in left side defects with right side defects untreated as negative controls. Mouse groups were defect only (n = 10), polydopamine-coated PLLA fibers (n = 10), fibers with 250 ng/mL immobilized BMP-2 (n = 10), and fibers with 500 ng/mL immobilized BMP-2 (n = 10). Surgery sites were sutured and treated with pobidone iodine. All mice were sacrificed after 2 months.

2.11. Soft X-ray and Micro-CT. Soft X-ray and micro-CT were used to determine new bone formation. Mice were sacrificed using CO2 gas and skull bones were extracted. Bone samples were fixed using 10% neutral formalin and stored at 4 ° C for 3 days. Samples were exposed to soft X-rays (CMP-2, Softex Co., Tokyo, Japan) under fixed conditions (23 kV, 2 mA, 90 s) and samples were chosen for micro-CT scanning (80 kV, 124 μA; Skyscan1172, Bruker-microct, Belgium) using the X-ray images. Three-dimensional images from micro-CT scanning were analyzed with Adobe Photoshop CS6 (Adobe Systems, CA, USA) to measure regenerated bone areas.

2.12. Histological Analysis. Samples were decalcified using Rapidcal for 2 weeks (BBC Biochemical, Mount Vernon, WA, USA) with solution replacement every 2 days. Samples were dehydrated with graded EtOH (70−100%), toluene, and paraffin. Dehydrated samples were embedded in paraffin wax and hardened into a paraffin block for sectioning. Specimens were cut to 6 μm using a microtome (Shandon, Runcorn, Cheshire, GB). Sections underwent deparaffinization and hydration and stained nuclei and cytosol with Harris hematoxylin and eosin solution. Goldner's trichrome staining method was used to determined detailed bone tissue morphology such as mineralized collagen. Following dehydration, samples were mounted with mounting medium (Richard-Allan Scientific, Kalamazoo, MI, USA) and observed under an optical microscope (Nikon 2000, Japan).

2.13. SEM and TEM Imaging of Bone Tissue with Implants. To observe interactions between implanted nanofibers and regenerated tissue, defects for nanofiber-implanted calvarias were cut in to a perpendicular cutting plane. SEM specimens were fixed with modified Karnovky's fixative (2% paraformaldehyde, 2% glutaraldehyde in 0.05 M sodium cacodylate buffer, pH 7.2) and 1% osmium tetroxide in 0.05 M sodium cacodylate buffer (pH 7.2). Fixed specimens were serially dehydrated with EtOH (30−100%) and completely dried using 100% hexamethyldisilazane. Specimens were placed on metal stubs and coated with gold using a sputter coater. Morphology was observed by FE-SEM (AURIGA, Carl Zeiss, Germany). Transmission electron microscopy (TEM) preparation was the same as for SEM. Transition steps used 100% propylene oxide at room temperature for 15 min and embedding was with Spurr's resin with polymerization at 70 °C for 24 h. Polymerized samples were sectioned by ultramicrotome (MT-X, RMC, Tucson, AZ, USA) and stained with 2% uranyl acetate and Reynolds' lead citrate for 7 min. Samples were observed by TEM (LIBRA 120, Carl Zeiss, Germany).

2.14. Statistical Analysis. Quantitation used triplicate samples and values were expressed as mean ± standard deviation. Statistical significance was determined using Student's t test and ANOVA. Statistical significance was defined as p-value less than 0.05.

3. RESULTS AND DISCUSSION

Synthetic polymers are promising candidates for biomedicine since their mechanical and chemical properties can be finely

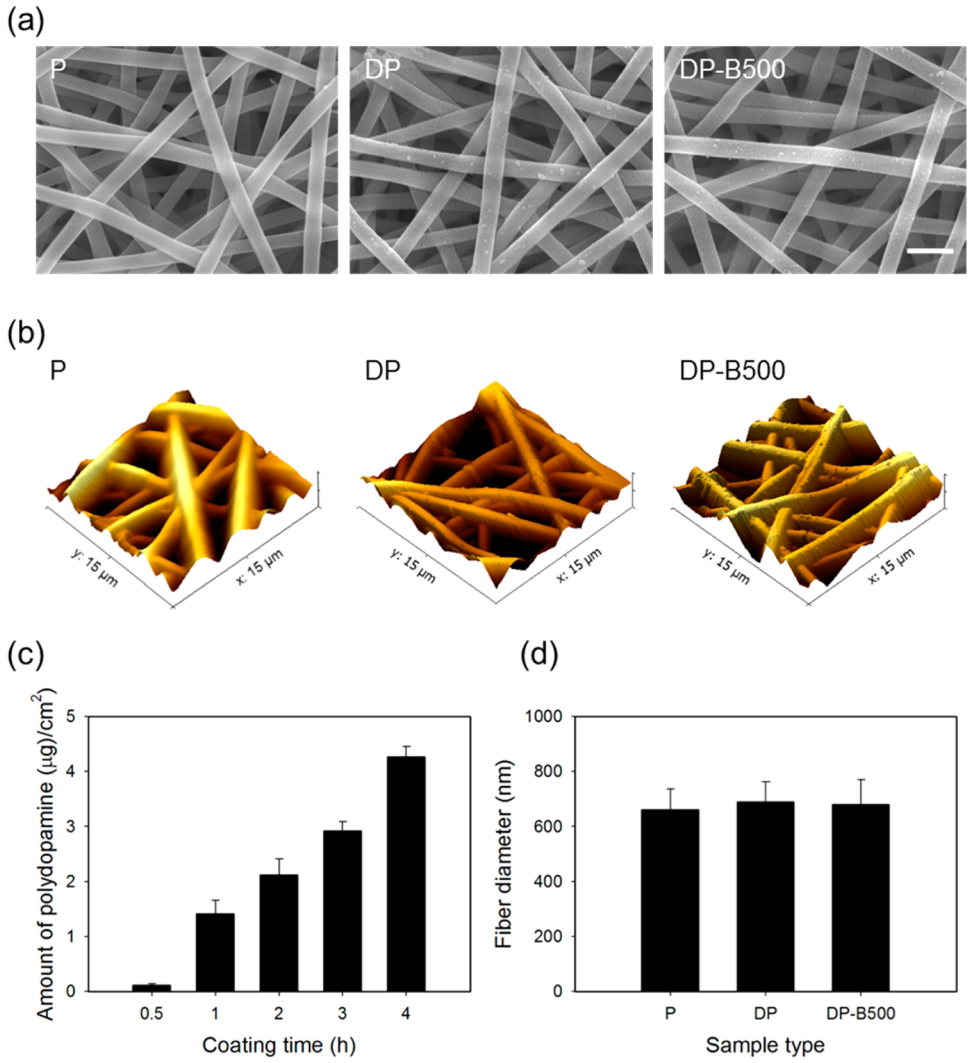

Figure 2. Characteristics of electrospun fibers. (a) SEM showing electrospun fiber morphology (scale bar = 2 μm). (b) Surface roughness of electrospun fibers characterized by AFM. (c) Amount of polydopamine on PLLA nanofibers by coating time. (d) Diameters of nanofibers before and after immobilization.

tuned. Among various poly(α-hydroxy esters), PLLA has shown a favorable degradation rate and mechanical properties for nanofiber-based tissue engineering applications.[19] However, the inability to produce required biological cues often limits their application in tissue engineering. In this study, osteoinductive electrospun PLLA nanofibers were fabricated by polydopamine coating and subsequent BMP-2 immobilization. Experimental groups were PLLA nanofibers (P), polydopamine-coated nanofibers (DP), polydopamine-coated nanofibers further immobilized with 250 ng/mL BMP-2 (DP-B250) and 500 ng/mL BMP-2 (DP-B500). Preparation of nanofibers with immobilized BMP-2 is shown in Figure 1.

3.1. Fabrication of Nanofiber Membranes with Immobilized BMP-2. We examined morphological differences between P, DP and DP-B500 samples. SEM revealed structural similarity among groups in nanofiber distribution, pore size and fiber diameter as shown in Figure 2a. AFM images were consistent with SEM analysis with incremental differences in surface roughness between samples coated with polydopamine and samples coated with BMP-2 (Figure 2b). These results were in agreement with our and others previous studies in which polydopamine-coated PLCL films and PLGA nanofibers showed relatively rougher surface morphology compared to uncoated polymer substrates.[20−22] As shown in Figure 2c, the amount of polydopamine on fiber surfaces increased from 0.12 ± 0.02 to 4.27 ± 0.19 μg/cm^2 as coating time increased from 30 min to 4 h. We previously reported that the amount of polydopamine coated on PLCL films was time dependent. However, the quantity of coated polydopamine on PLCL films and PLLA nanofibers was different, possibly because of surface area differences. Differences in surface energy between PLCL and PLLA could also affect the amount of coated polydopamine. Collectively, these results indicated that the amount of polydopamine coating could be controlled by adjusting coating time. No significant difference was observed in the average fiber diameter in the P (662 ± 74 nm), DP (689 ± 73 nm), or DP-B500 (680 ± 90 nm) groups (Figure 2d), which was similar to a previous study.[17]

3.2. Surface Chemical Compositions of Fiber Membrane. Surface chemical compositions were verified using XPS spectra for P, DP, and DP-B500 samples (Figure 3a−c). Representative spectra for carbon (C 1s) (288 eV) and oxygen (O 1s) (533 eV) were found on all PLLA nanofiber surfaces, but nitrogen (N 1s) peak (399 eV) was seen only for

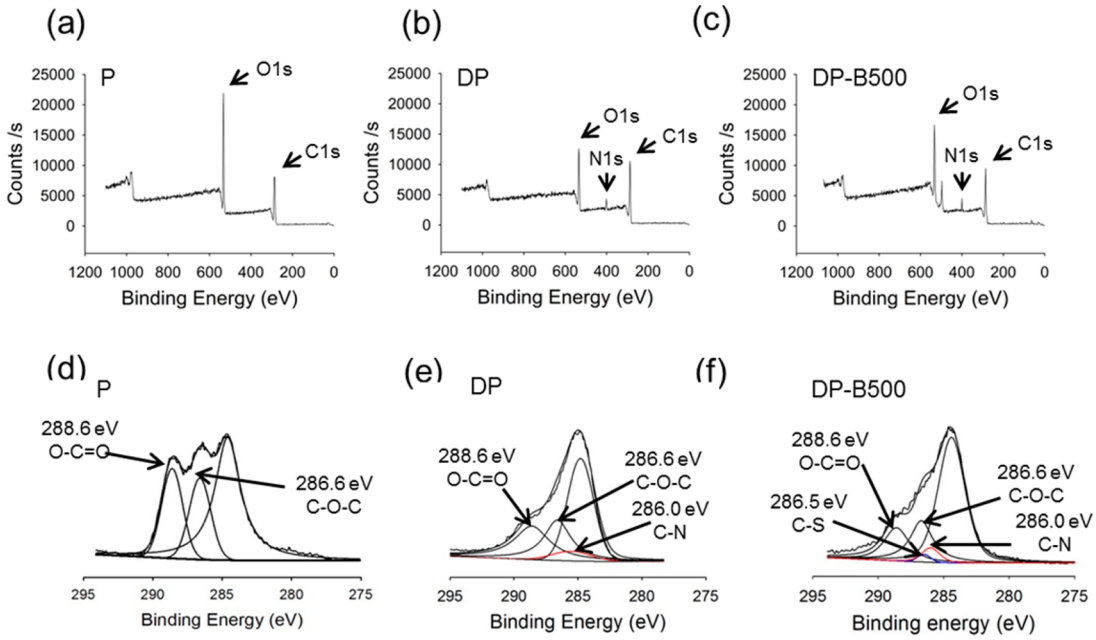

Figure 3. Surface chemical composition of nanofibers. XPS spectra from (a) P, (b) DP, and (c) DP-B500 nanofibers. High-resolution spectra of carbon peak C 1s on (d) P, (e) DP, and (f) DP-B500 nanofibers. Individual peaks from different carbon bonding are assigned and summation curve is also included.

polydopamine-coated nanofibers and nanofibers with immobilized BMP-2. High-resolution carbon spectrum analysis showed the presence of C−O−C (286.6 eV) and O−C═O (288.6 eV) peaks for all samples which are present in the PLLA chain.[23,24] Presence of C−N (286.0 eV) spectra were only observed on the modified surfaces of DP and DP-B500 samples, as found in previous studies.[11,25] Presence of C−O−C and O−C═O were also observed in the polydopamine modified groups with reduced intensity indicating that surface of PLLA is little exposed ever after polydopamine coating. Appearance of O−C═O peaks in DP-B 500 groups can also be attributed to COOH groups of BMP-2. The intensity of the C−N spectra was higher for surfaces with immobilized BMP-2 than DP surfaces. A small C−S (286.5 eV) spectrum peak associated with BMP-2 immobilization was also found for DP-500 samples (Figure 3d−f). We have also calculated the N/C values and found that N/C values were increased by 1.43-fold for nanofibers with immobilized BMP-2 (0.10) compared to nanofibers coated with polydopamine only (0.07) and pristine nanofiber groups (0). This can be ascribed to introduction of amine groups by polydopamine coating and further increase in the N/C values in the BMP-2 immobilized groups is evident for the incorporation of primary amines and amide bonds by the immobilized protein. Our previous results showed that polydopamine coating enhanced the intensity of C−N peaks compared to controls.[20,21] A few earlier reports used XPS to analyze ad-layers of BMP-2 immobilized on a polydopamine-coated substrate showing increased N 1s intensity when BMP-2 was immobilized on polydopamine-coated substrates.[26,27] These results suggested that PLLA nanofibers were efficiently modified with polydopamine coating and immobilized BMP-2.

Recently, polydopamine-mediated surface immobilization of growth factors on synthetic substrates for tissue engineering applications have shown lot of promises. It was believed that Schiffs base reactions or Michael addition between thiol or amine group of biomolecules and catechol/quinone groups of the polydopamine coated substrates may be responsible for the immobilization of biomolecules.[28,11] In one of the studies, VEGF was successfully immobilized on polydopamine coated metal surface which was confirmed by surface chemical analysis and enhanced differentiation of hMSCs to endothelial cells.[29] Lai, Min et.al., has immobilized BMP-2 on titanium nanotubes, which has been efficiently used for osteogenic differentiation of mesenchymal stem cells.[30] Similarly, BMP-2 was immobilized along with cell adhesive peptides and hydroxyapatite on titanium, and showed improved osteogenis of bone marrow stem cells.[31] In a previous attempt from our laboratory, we have successfully conjugated bone forming peptide-1 derived from BMP-7 on an electrospun nanofibers and used it for guided bone regeneration in an in vivo mouse model.[17] In general, lots of attempts have shown the effective polydopmine mediated immobilization of growth factors for tissue engineering applications. However, the actual mechanisms on how growth factors react with polydopamine have yet to be discovered and there is a lack of adequate research in that direction, which definitely requires further investigation.

3.3. Quantification of Immobilized BMP-2. We indirectly measured the amount of BMP-2 on nanofibers.[16] The amount of immobilized BMP-2 on polydopamine-coated nanofibers increased as the concentration of BMP-2 in treatment solutions increased (Figure 4a). When 500 μL of BMP-2 at 250 ng/mL or 500 ng/mL was used to treat 1 cm^2 of polydopamine-coated nanofibers, the DP-B500 group showed more immobilized BMP-2 (124 ± 9 ng/cm^2) than the DP-250 group (61 ± 8 ng/cm^2). These results matched findings on the amount of BMP-2 immobilized on to O_2 plasma-treated polystyrene surfaces (44.2 ng/cm^2) and gold surfaces modified by self-assembled monolayer formation (70−80 ng/cm^2).[32,33] In this study, BMP-2 immobilization efficiency was approximately 80% in both groups. This high efficiency was comparable to previous reports on immobilization of RGD peptide (80%) and glial cell line-derived neurotrophic factor (90%) on polydopamine-coated polystyrene substrates, and

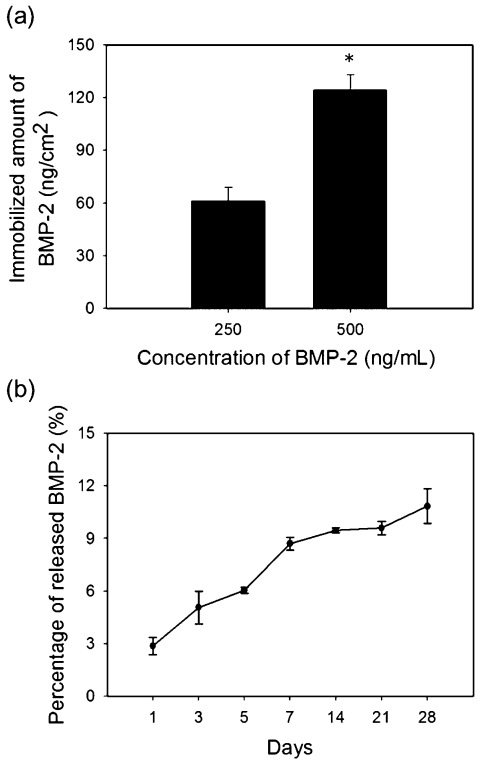

Figure 4. Quantification of BMP-2 immobilized on polydopamine-coated nanofibers using ELISA. (a) Amount of immobilized BMP-2 on fibers prepared using different BMP-2 concentrations. "*" represents significant difference between the group with 500 ng/mL immobilized BMP-2 group and the group with 250 ng/mL immobilized BMP-2 ($p < 0.05$). (b) Percentage of released BMP-2 from the nanofiber at different time periods under physiological condition (PBS, 37 °C).

immobilization of BMP-2 on chitosan-grafted titanium surfaces (81%).[34,35]

Retention of Immobilized BMP-2 on Polydopamine Coated Nanofibers. We then investigated the retention of BMP-2 on polydopamine coated nanofibers for up to 28 days. We restricted this study to DP-B500 groups and it was observed that approximately 90% of the immobilized BMP-2 was retained on the surface of nanofibers at the end of 28 days with minimal initial burst release (Figure 4b). During the 28 days of in vitro release study, around 9% of the BMP-2 release was observed at initial 7 days and only 2% of BMP-2 was released during day 7 to day 28. These results clearly show that most of BMP-2 was stably retained as immobilized on nanofibers. We assume that initial release of approximately 9% of total immobilized BMP-2 may be attributed to the physical adsorption onto polydopamined-coated nanofibers. These results are consistent with previous works from our and other laboratory, in which immobilized RGD or bFGF on polydopamine-coated PLCL films showed greater than 90% retention efficiency over 6 h.[16] Another study immobilized catalase enzyme on polydopamine microcapsules and found low leakage ratio of 6% over 8 h.[36] On the other hand, when BMP-2 peptide was conjugated with hydroxyapatite on a titanium alloy, 25% of the initial amount of BMP-2 was released during first 7 days of incubation in PBS.[37] In another approach, appetite-coated chitosan scaffolds were used to load BMP-2 and 18% of the initial loaded BMP-2 was released from the appetite substrate at day one.[38] An ideal growth factor delivery systems should control the initial burst release as it might reduce the dose required for tissue regeneration and also avoids the concerns regarding its safety and expenses. Though there have been previous reports on effective immobilization of biomolecules using polydopamine, there long-term release behavior was not well characterized. As mentioned earlier, our developed nanofiber by immobilizing BMP-2 using polydopamine was effective in terms of retention on the fibers as evident from long-term release assays and this method was superior to many recently reported approaches. Almost 80% of immobilized BMP-2 was released from an heparin-conjugated fibrin delivery system within 1 month of incubation as reported by Yang, Hee Seok et al.[39] In another approach, VEGF was loaded on genipin cross-linked electrospun gelatin nanofibers and more than 50% of the immobilized VEGF was lost during the incubation period of 1 month.[40] Sintered polymer scaffolds were developed and used for BMP-2 delivery; however, 60% of BMP-2 was released after 3 weeks of time.[41] In a recent report, long-term release behavior of immobilized BMP-2 was analyzed over a period of 28 days from a polydopamine coated titanium surface and which showed excellent retention of growth factor even after 1 month.[42] To the best of our knowledge, we are reporting first time of a long-term release behavior of BMP-2 from a polydopamine-coated fibrous polymeric membrane. Long-term retention of immobilized growth factor is particularly relevant in the context of guided bone regeneration approaches, as the porous membrane expected to provide osteoinductivity for relatively longer period. We assume a similar release behavior of BMP-2 from our nanofiber membrane in in vivo environments; however, further analysis may be needed for understanding the conformational changes and structure of immobilized biomolecules after implantation, which would be a consideration in our future approaches.

3.4. Enhanced in Vitro Osteogenic Differentiation of hMSCs on BMP-2 Immobilized Nanofibers. The cell morphology of hMSCs cultured on electrospun fibers for 1 or 14 days in osteogenic medium was characterized by immunofluorescence. On unmodified PLLA nanofibers, the hMSCs showed limited cell adhesion and spreading at 1 day and restricted proliferation at 14 days. DP and DP-B500 supported stable cell attachment and wide cell coverage as well as active cell growth at 1 and 14 days (Figure 5a, b). These observations were consistent with our previous studies in which polydopamine coating improved the hydrophilicity of synthetic polymer substrates, resulting in improved proliferation of C2C12, HUVEC, and hMSCs.[16,17,20]

We used SEM to analyze the surface morphology of hMSCs cultured on nanofibers for 14 days (Figure 5c). The surface of hMSCs cultured on PLLA nanofibers was smooth and clear, whereas cells cultured on modified surfaces had a rougher surface morphology, indicating more extracellular matrix secretion. These results were similar to our previous studies in which hydroxyapatite or BFP1-containing synthetic polymer nanofibers enhanced osteogenic differentiation and mineralization of hMSCs.[17,43] To examine the potential of BMP-2 immobilized on fibers to induce osteogenic differentiation of hMSCs, we measured ALP activity and calcium amounts (Figure 6a and 6b). The ALP activity of hMSCs cultured on DP-B500 (2.3 ± 0.2 nmol/DNA/30 min) was significantly higher than that in other culture groups. hMSCs cultured on DP-B250 (1.8 ± 0.1 nmol/DNA/30 min) and DP (1.6 ± 0.2 nmol/DNA/30 min) had significantly greater ALP activity than hMSCs in the P group (1.1 ± 0.2 nmol/DNA/30 min). These results were similar to calcium assay results (Figure 6b). The

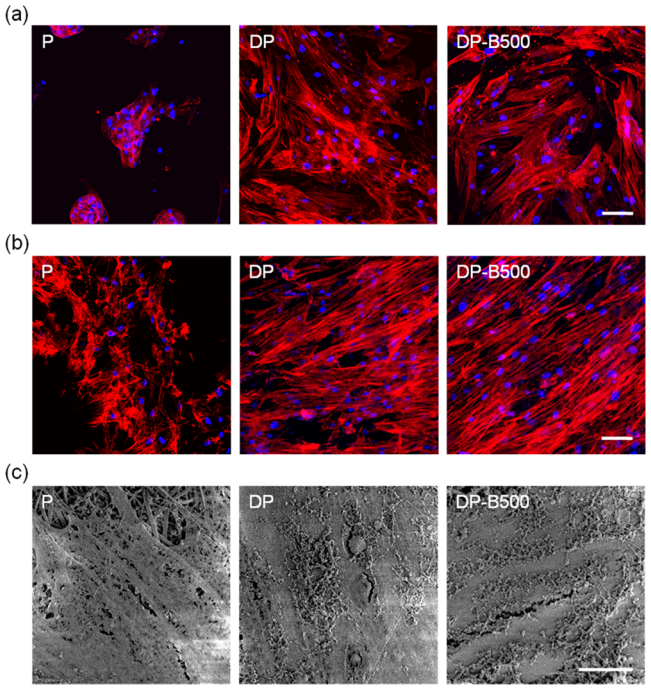

Figure 5. Morphology of hMSCs cultured on nanofibers. Fluorescence images of staining for f-actin (red) and nuclei (blue) in hMSCs cultured for (a) 1 day or (b) 14 days on P, DP, or DP-B500 nanofibers (scale bar = 100 μm). (c) SEM images analyzing ECM secretion of hMSCs cultured for 14 days on different types of electrospun fibers (scale bar = 10 μm).

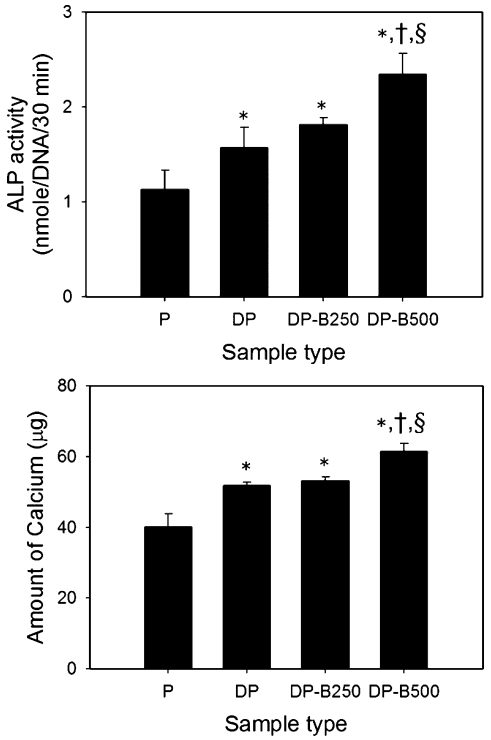

Figure 6. Osteogenic differentiation of hMSCs cultured on different nanofibers. (a) ALP activity of hMSCs on P, DP, DP-B250, and DP-B500 nanofibers for 10 days. (b) Quantification of mineralized calcium from hMSCs cultured on different nanofibers for 14 days. "*" represents significant difference compared to P group; "†" represents significant difference compared to DP group; and "§", significant difference compared to the DP-B250 group ($p < 0.05$).

amount of mineralized calcium in hMSCs cultured on DP-B500 (61.5 ± 2.2 μg) was significantly increased compared to other groups. Mineralized calcium levels were similar for hMSCs cultured on DP-B250 (53.2 ± 1.0 μg) and DP (51.9 ± 0.9 μg) nanofibers, but higher than calcium mineralization in hMSCs on PLLA nanofibers (40.1 ± 3.8 μg). The effective concentration of immobilized BMP-2 was comparable to the concentration reported in Shi, et al. in which 146 ± 19 ng/cm^2 BMP-2 immobilized on a titanium substrate enhanced osteogenic differentiation of hMSCs compared to a group of hMSCs cultured with 28 ± 8 ng/cm^2 immobilized BMP-2. No significant difference was seen in ALP activity between a group of cells cultured for 1 week with 28 ± 8 ng/cm^2 immobilized BMP-2 and cells cultured on other modified surfaces.[44] Collectively, these results suggest that there should be a minimum concentration of chemical stimulus to enhance the cell functions.

3. 5. Enhanced in Vivo Bone Formation by DP-B500 PLLA Nanofibers. We implanted nanofibers in a calvarial critical size defect mouse model and analyzed *in vivo* bone formation (Figure 7). Soft X-ray images showed enhanced bone regeneration in groups of mice implanted with surface-modified nanofibers compared to little detection of bone formation in the defect-only group (Figure 7a). The results were reconfirmed by three-dimensional micro-CT images, which showed more detailed regenerated bone (Figure 7b and 7c). Analysis revealed limited bone regeneration (5.9 ± 1.0%) in the defect-only group, while DP-B500 nanofiber-implanted groups showed significantly accelerated bone regeneration (77.8 ± 11.7%). Mice in the DP-B250-implanted and DP-implanted groups showed similar bone regeneration (38.0 ± 7.1% and 34.1 ± 5.5%) with enhanced bone regeneration compared to the defect-only group. These results were consistent with in vitro experiment results. The amount of immobilized BMP-2 implanted into each defect was 25 ng for DP-B500 nanofibers and 12 ng for DP-B250 nanofibers, which was significantly lower than BMP-2 used in previous studies. In several studies of BMP-2-release strategies, several hundred nanogram to a several microgram of BMP-2 was required for effective bone formation, particularly when tested in calvarial critical size defect mouse models.[45,46] High dosage BMP-2 may have issues associated with its side effects or cost effectivelessness.[47] Resent researches are focusing on lowering the dosage of immobilized BMP-2. In one of the very recent attempts, Rahman et.al loaded 1 μg of BMP-2 with PLGA/PEG scaffolds into mouse calvarial model and achieved 55% of new bone area compared to a defect only group after 6 weeks of implantation.[41] In our approach, we achieved almost 80% of new bone regenerated area using 25 ng of loaded BMP-2 after 8 weeks of implantation which is several fold lower than previously mentioned approaches. To the best of our knowledge, this is one of the lowest dosages of BMP-2 which resulted in satisfactory level of bone regeneration in a mouse calvarial defect model. Our results suggest that polydopamine mediated immobilization of BMP-2 using a simple method reduced the dose by stable and localized delivery of BMP-2 at the defect site.

3.6. Maturation of Newly Formed Bone on BMP-2 Immobilized Nanofiber Groups. Histological analysis was used to observe interactions between host tissue and implanted nanofibers at defect sites (Figure 8a). Mice in the nanofiber-implanted group showed thicker, more organized tissue regeneration throughout the defect sites than mice in the

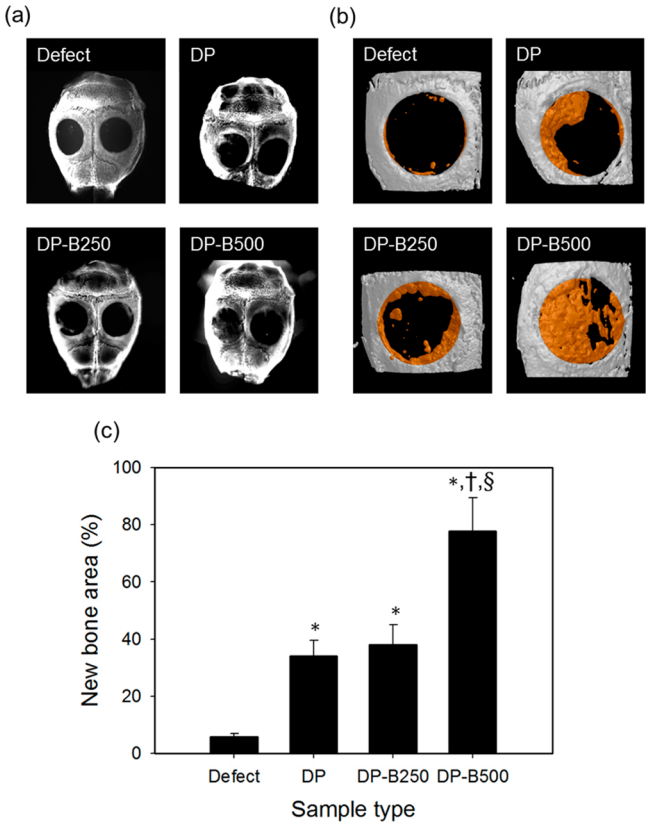

Figure 7. Radiographic analysis of skull bones implanted with nanofibers at two months after surgery. Skull bone samples with implanted nanofibers were analyzed by (a) soft X-ray and (b) micro-CT. (c) Regenerated new bone area from micro-CT images. "*" represents significant difference compared to the defect-only group; "†"represents significant difference as compared to the DP group; and "§"represents significant difference compared to the DP-B250 group ($p < 0.05$). Nanofibers were implanted only in defects on the left side.

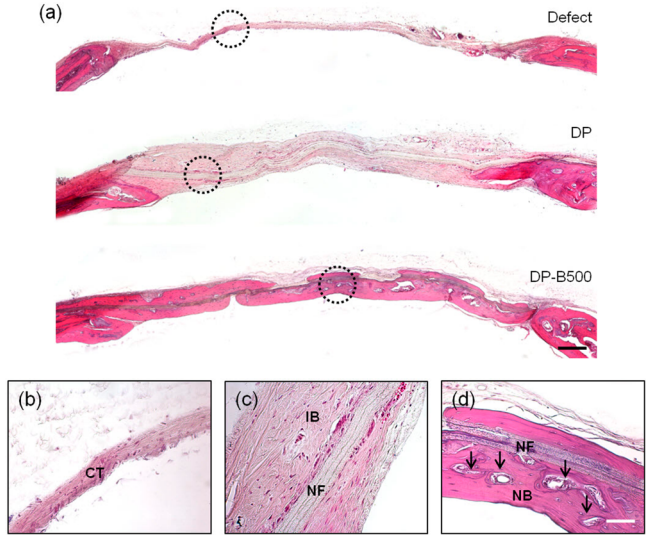

Figure 8. H&E staining of sectioned mouse calvarial defect samples after two months of nanofiber implantation. (a) Defect only, DP, and DP-B500. (b) Defect only, (c) DP, and (d) DP-B500 are magnified images (400x) of the dotted portions from each group (scale bar = 50 μm). Black arrows, newly generated blood vessels in regenerated bone (CT = connective tissue, NF = nanofiber, IB = immature bone, NB = new bone).

defect-only group (Figure 8b). In mice in the DP-implanted group, nanofibers were encapsulated with host cells and tighter tissue formation along the fibers was detected (Figure 8c). Mice in the DP-B500-implanted group showed compact bone formation and fiber degradation caused by tissue infiltration, and regeneration of blood vessels (black arrow) underneath the implanted membrane (Figure 8d). Goldner's trichrome staining indicated tight distribution of regenerated collagen tissues and partially regenerated bone at the center of defect sites implanted with DP nanofibers (Figure 9a). Mice in the DP-

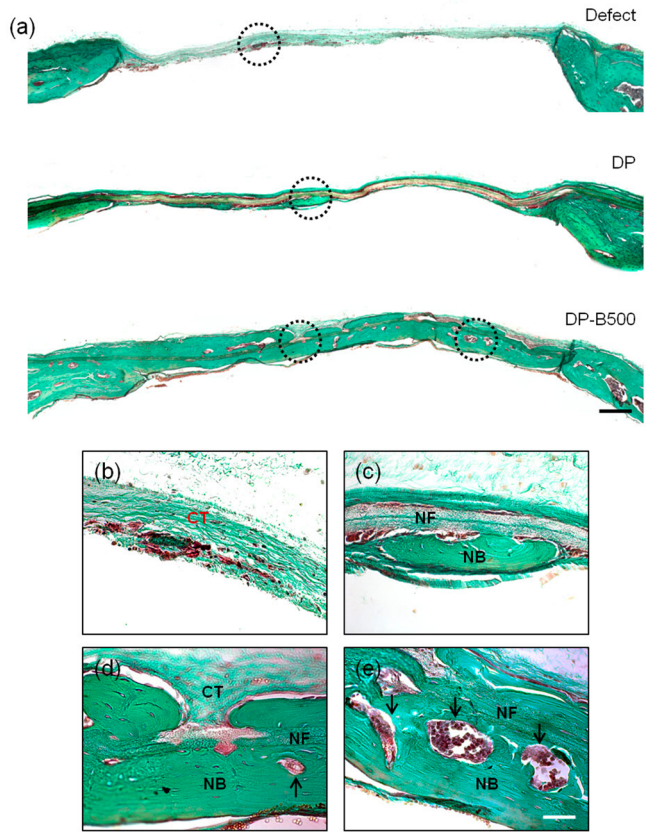

Figure 9. Goldner's trichrome histological images of sectioned nanofiber-implanted calvarial models after two months of implantation. (a) Defect only, DP and DP-B500 samples showing whole cross-sectioned planes. (b) Defect only, (c) DP, and (d, e) DP-B500 (400×) are magnified images of dotted portions of images (scale bar = 50 μm). Black arrows, newly generated blood vessels within the regenerated bone (CT = connective tissue, NF = nanofiber, NB = new bone).

B500-implanted group showed thick, mature bone formation throughout the defect area and regenerated tissue that was completely integrated with host bone tissue at the defect edge. Higher magnification histological images of mice in the defect-only group showed regenerated connective tissues that were compared of nonwoven collagen tissues (Figure 9b). Mice in the DP and DP-B500 groups showed an increase in the quality of packed collagen tissues and amount of matured bone tissue compared to other groups (Figure 9c, d). Mice in the DP-B500-implanted group showed the most fiber degradation of all groups, suggesting active tissue infiltration into the nanofibers. Large blood vessels (black arrow) and lacunae were observed throughout the regenerated tissue, indicating maturation of newly formed bone at the defect sites (Figure 9d, e). Comparable results were observed in previous experiments in

which the efficiency of chitosan nanofibers for bone regeneration was examined over 4 weeks in a rabbit calvarial defect model. In another approach, the effects of polytetrafluoroethylene, polyglactin, and collagen membranes were compared for bone formation for 60 days after surgery using rat cranial defects.[48,49] However, histological staining showed immature newly formed bone, limited tissue integration, and little scaffold collapse at defect sites. In contrast, in our results, mice implanted with DP-B500 showed thick, mature bone tissue formation even on the upper side of the nanofibers. Our results indicated that polydopamine-mediated immobilization of BMP-2 on fibers efficiently induced in vitro osteogenic differentiation and in vivo bone regeneration with enhanced maturation of newly formed bone tissues.

3.7. Active Collagen Deposition on Implanted BMP-2 Immobilized Nanofibers. We used SEM and TEM perpendicular to the defect site in mice implanted with DP-B500 to analyze surface interactions between regenerated tissue and implanted nanofibers (Figure 10a). Thick regenerated collagen fibers were observed along the bottom of the implanted nanofibers. Collagen is the most abundant protein in bone and might be able to transform into new bone tissue. TEM clearly showed fibroblasts and osteoblasts with nanofiber strands in the middle of regenerated bone tissue.[50] Fibroblast-secreting collagen fibrils were found in spaces between nanofiber strands oriented toward the defect sites (Figure 10b, c). We also observed coated polydopamine on nanofibers (white arrow) and collagen fibril distribution occurred around the polydopamine-coated nanofibers without definite orientation (Figure 10d). Our results suggest that the coated polydopamine layer was stably maintained for two months in vivo and implanted nanofiber surface interacted sufficiently with host cells and the extracellular environment.

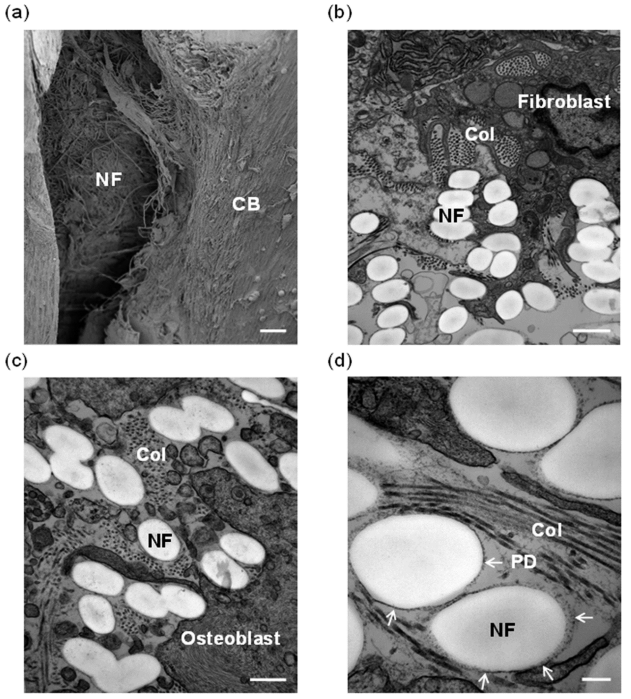

Figure 10. (a) SEM (scale bar = 10 μm) and (b–d) TEM micrographs of calvaria tissues implanted with DP-B500 nanofibers, two months after surgery (scale bar = 1 μm, 0.5 μm, 20 nm). White arrows indicate polydopamine-coated layer on PLLA nanofibers (NF = implanted nanofiber, CB = collagen fibril bundle arranged along the random structure of nanofibers, Col = collagen fibrils secreted from fibroblasts, PD = polydopamine layer).

4. CONCLUSIONS

In this study, we developed and characterized a biodegradable nanofiber immobilized with BMP-2 using polydopamine chemistry for guided bone regeneration. Surface chemical characterization demonstrated that polydopamine coating and BMP-2 immobilization were successful. Quantification of BMP-2 on membranes showed that immobilized BMP-2 increased with increasing concentrations of BMP-2 in treatment solutions. Notably, long-term release analysis of BMP-2 from the naofibers showed the effective retention of the immobilized BMP-2 as about 90% of the immobilized BMP-2 was retained even after one month of incubation time at in vitro physiological conditions. Studies with hMSCs demonstrated enhanced initial cell adhesion, proliferation, and osteogenic differentiation of hMSCs cultured on fibers modified with BMP-2. Moreover, a calvarial critical size defect mouse model implanted with fibers with immobilized BMP-2 showed improved bone formation compared to a control group. Our fibers with 124 ± 9 ng/cm^2 immobilized BMP-2 gave results superior to those reported in other studies for both in vitro osteogenic differentiation and in vivo bone formation, while using a relatively smaller amount of BMP-2. Together, our results suggested that polydopamine-mediated BMP-2 immobilization on nanofibers might be a feasible method for effective delivery of osteoinductive signals for guided bone regeneration.

AUTHOR INFORMATION

Corresponding Authors

*E-mail: cshin@sogang.ac.kr. Tel.: +82-2-705-8825. Fax: +82-2-712-0799.

*E-mail: hshin@hanyang.ac.kr. Tel.: +82-2-2220-2346. Fax: +82-2-2298-2346 .

Author Contributions

†Authors H.-j.C. and S.K.M.P. contributed equally. The manuscript was written through contributions of all authors. All authors have given approval to the final version of the manuscript.

Funding

This work was supported by the National Research Foundation of Korea (NRF) grant funded by the Korea government (MEST) (2013R1A2A2A03067809 and 2012K001418).

Notes

The authors declare no competing financial interest.

REFERENCES

(1) Mellonig, J. T.; Nevins, M. Guided Bone Regeneration of Bone Defects Associated with Implants: An Evidence-Based Outcome Assessment. *Int. J. Periodontics Restor. Dent.* **1995**, *15*, 168–185.

(2) Pham, Q. P.; Sharma, U.; Mikos, A. G. Electrospinning of Polymeric Nanofibers for Tissue Engineering Applications: A Review. *Tissue Eng.* **2006**, *12*, 1197–1211.

(3) Li, X.; Xie, J.; Yuan, X.; Xia, Y. Coating Electrospun Poly(Epsilon-Caprolactone) Fibers with Gelatin and Calcium Phosphate and Their Use as Biomimetic Scaffolds for Bone Tissue Engineering. *Langmuir* **2008**, *24*, 14145–14150.

(4) Mavis, B.; Demirtas, T. T.; Gumusderelioglu, M.; Gunduz, G.; Colak, U. Synthesis, Characterization and Osteoblastic Activity of Polycaprolactone Nanofibers Coated with Biomimetic Calcium Phosphate. *Acta Biomater.* **2009**, *5*, 3098–3111.

(5) Seyedjafari, E.; Soleimani, M.; Ghaemi, N.; Shabani, I. Nanohydroxyapatite-Coated Electrospun Poly(L-Lactide) Nanofibers Enhance Osteogenic Differentiation of Stem Cells and Induce Ectopic Bone Formation. *Biomacromolecules* **2010**, *11*, 3118−3125.
(6) Zhang, Q.; He, Q. F.; Zhang, T. H.; Yu, X. L.; Liu, Q.; Deng, F. L. Improvement in the Delivery System of Bone Morphogenetic Protein-2: A New Approach to Promote Bone Formation. *Biomed Mater.* **2012**, *7*, 045002.
(7) Kim, J. E.; Lee, E. J.; Kim, H. E.; Koh, Y. H.; Jang, J. H. The Impact of Immobilization of BMP-2 on PDO Membrane for Bone Regeneration. *J. Biomed. Mater. Res.,Part A* **2012**, *100*, 1488−1493.
(8) Kim, S. E.; Song, S. H.; Yun, Y. P.; Choi, B. J.; Kwon, I. K.; Bae, M. S.; Moon, H. J.; Kwon, Y. D. The Effect of Immobilization of Heparin and Bone Morphogenic Protein-2 (BMP-2) to Titanium Surfaces on Inflammation and Osteoblast Function. *Biomaterials* **2011**, *32*, 366−373.
(9) Luginbuehl, V.; Meinel, L.; Merkle, H. P.; Gander, B. Localized Delivery of Growth Factors for Bone Repair. *Eur. J. Pharm. Biopharm.* **2004**, *58*, 197−208.
(10) Lee, H.; Dellatore, S. M.; Miller, W. M.; Messersmith, P. B. Mussel-Inspired Surface Chemistry for Multifunctional Coatings. *Science* **2007**, *318*, 426−430.
(11) Lee, H.; Rho, J.; Messersmith, P. B. Facile Conjugation of Biomolecules onto Surfaces Via Mussel Adhesive Protein Inspired Coatings. *Adv. Mater.* **2009**, *21*, 431−434.
(12) Lynge, M. E.; van der Westen, R.; Postma, A.; Stadler, B. Polydopamine–a Nature-Inspired Polymer Coating for Biomedical Science. *Nanoscale* **2011**, *3*, 4916−4928.
(13) Luo, R.; Tang, L.; Wang, J.; Zhao, Y.; Tu, Q.; Weng, Y.; Shen, R.; Huang, N. Improved Immobilization of Biomolecules to Quinone-Rich Polydopamine for Efficient Surface Functionalization. *Colloids Surf., B* **2013**, *106*, 66−73.
(14) Jeong, C. G.; Zhang, H.; Hollister, S. J. Three-Dimensional Polycaprolactone Scaffold-Conjugated Bone Morphogenetic Protein-2 Promotes Cartilage Regeneration from Primary Chondrocytes in Vitro and in Vivo without Accelerated Endochondral Ossification. *J. Biomed. Mater. Res., Part A* **2012**, *100*, 2088−2096.
(15) Shin, Y. M.; Lee, Y. B.; Kim, S. J.; Kang, J. K.; Park, J. C.; Jang, W.; Shin, H. Mussel-Inspired Immobilization of Vascular Endothelial Growth Factor (VEGF) for Enhanced Endothelialization of Vascular Grafts. *Biomacromolecules* **2012**, *13*, 2020−2028.
(16) Lee, Y. B.; Shin, Y. M.; Lee, J. H.; Jun, I.; Kang, J. K.; Park, J. C.; Shin, H. Polydopamine-Mediated Immobilization of Multiple Bioactive Molecules for the Development of Functional Vascular Graft Materials. *Biomaterials* **2012**, *33*, 8343−8352.
(17) Lee, Y. J.; Lee, J. H.; Cho, H. J.; Kim, H. K.; Yoon, T. R.; Shin, H. Electrospun Fibers Immobilized with Bone Forming Peptide-1 Derived from BMP 7 for Guided Bone Regeneration. *Biomaterials* **2013**, *34*, 5059−5069.
(18) Slocum, T. L.; Deupree, J. D. Interference of Biogenic Amines with the Measurement of Proteins Using Bicinchoninic Acid. *Anal. Biochem.* **1991**, *195*, 14−17.
(19) Li, W.-J.; Cooper, J. A., Jr; Mauck, R. L.; Tuan, R. S. Fabrication and Characterization of Six Electrospun Poly (A-Hydroxy Ester)-Based Fibrous Scaffolds for Tissue Engineering Applications. *Acta Biomater.* **2006**, *2*, 377−385.
(20) Shin, Y. M.; Lee, Y. B.; Shin, H. Time-Dependent Mussel-Inspired Functionalization of Poly(L-Lactide-Co-Varepsilon-Caprolactone) Substrates for Tunable Cell Behaviors. *Colloids Surf., B* **2011**, *87*, 79−87.
(21) Rim, N. G.; Kim, S. J.; Shin, Y. M.; Jun, I.; Lim, D. W.; Park, J. H.; Shin, H. Mussel-Inspired Surface Modification of Poly(L-Lactide) Electrospun Fibers for Modulation of Osteogenic Differentiation of Human Mesenchymal Stem Cells. *Colloids Surf., B* **2012**, *91*, 189−197.
(22) Ko, E.; Yang, K.; Shin, J.; Cho, S. W. Polydopamine-Assisted Osteoinductive Peptide Immobilization of Polymer Scaffolds for Enhanced Bone Regeneration by Human Adipose-Derived Stem Cells. *Biomacromolecules* **2013**, *14*, 3202−3213.
(23) Ma, Z.; Gao, C.; Gong, Y.; Ji, J.; Shen, J. Immobilization of Natural Macromolecules on Poly-L-Lactic Acid Membrane Surface in Order to Improve Its Cytocompatibility. *J. Biomed. Mater. Res.* **2002**, *63*, 838−847.
(24) Liu, W.; Zhan, J.; Su, Y.; Wu, T.; Wu, C.; Ramakrishna, S.; Mo, X.; Al-Deyab, S. S.; El-Newehy, M. Effects of Plasma Treatment to Nanofibers on Initial Cell Adhesion and Cell Morphology. *Colloids Surf., B* **2014**, *113*, 101−106.
(25) Zhu, L. P.; Jiang, J. H.; Zhu, B. K.; Xu, Y. Y. Immobilization of Bovine Serum Albumin onto Porous Polyethylene Membranes Using Strongly Attached Polydopamine as a Spacer. *Colloids Surf., B* **2011**, *86*, 111−118.
(26) Lee, D. W.; Yun, Y. P.; Park, K.; Kim, S. E. Gentamicin and Bone Morphogenic Protein-2 (BMP-2)-Delivering Heparinized-Titanium Implant with Enhanced Antibacterial Activity and Osteointegration. *Bone* **2012**, *50*, 974−982.
(27) Zheng, D.; Neoh, K. G.; Shi, Z.; Kang, E. T. Assessment of Stability of Surface Anchors for Antibacterial Coatings and Immobilized Growth Factors on Titanium. *J. Colloid Interface Sci.* **2013**, *406*, 238−246.
(28) LaVoie, M. J.; Ostaszewski, B. L.; Weihofen, A.; Schlossmacher, M. G.; Selkoe, D. J. Dopamine Covalently Modifies and Functionally Inactivates Parkin. *Nat. med.* **2005**, *11*, 1214−1221.
(29) Poh, C. K.; Shi, Z.; Lim, T. Y.; Neoh, K. G.; Wang, W. The Effect of Vegf Functionalization of Titanium on Endothelial Cells in Vitro. *Biomaterials* **2010**, *31*, 1578−1585.
(30) Lai, M.; Cai, K.; Zhao, L.; Chen, X.; Hou, Y.; Yang, Z. Surface Functionalization of Tio2 Nanotubes with Bone Morphogenetic Protein 2 and Its Synergistic Effect on the Differentiation of Mesenchymal Stem Cells. *Biomacromolecules* **2011**, *12*, 1097−1105.
(31) Chien, C.-Y.; Tsai, W.-B. Poly (Dopamine)-Assisted Immobilization of Arg-Gly-Asp Peptides, Hydroxyapatite, and Bone Morphogenic Protein-2 on Titanium to Improve the Osteogenesis of Bone Marrow Stem Cells. *Acs. Appl. Mater. Interfaces* **2013**, *5*, 6975−6983.
(32) Matsuzaka, K.; Yoshinari, M.; Kokubu, E.; Shimono, M.; Inoue, T. Behavior of Osteoblast-Like Cells on Fibronectin or Bmp-2 Immobilized Surface. *Biomed. Res. Tokyo* **2004**, *25*, 263−268.
(33) Pohl, T. L.; Boergermann, J. H.; Schwaerzer, G. K.; Knaus, P.; Cavalcanti-Adam, E. A. Surface Immobilization of Bone Morphogenetic Protein 2 Via a Self-Assembled Monolayer Formation Induces Cell Differentiation. *Acta Biomater.* **2012**, *8*, 772−780.
(34) Yang, K.; Lee, J. S.; Kim, J.; Lee, Y. B.; Shin, H.; Um, S. H.; Kim, J. B.; Park, K. I.; Lee, H.; Cho, S. W. Polydopamine-Mediated Surface Modification of Scaffold Materials for Human Neural Stem Cell Engineering (Vol 33, Pg 6952, 2012). *Biomaterials* **2012**, *33*, 8186−8187.
(35) Lim, T. Y.; Wang, W.; Shi, Z.; Poh, C. K.; Neoh, K. G. Human Bone Marrow-Derived Mesenchymal Stem Cells and Osteoblast Differentiation on Titanium with Surface-Grafted Chitosan and Immobilized Bone Morphogenetic Protein-2. *J. Mater. Sci. Mater. Med.* **2009**, *20*, 1−10.
(36) Shi, J.; Yang, C.; Zhang, S.; Wang, X.; Jiang, Z.; Zhang, W.; Song, X.; Ai, Q.; Tian, C. Polydopamine Microcapsules with Different Wall Structures Prepared by a Template-Mediated Method for Enzyme Immobilization. *ACS. Appl. Mater. Interfaces* **2013**, *5*, 9991−9997.
(37) Cai, Y.; Wang, X.; Poh, C. K.; Tan, H. C.; Soe, M. T.; Zhang, S.; Wang, W. Accelerated Bone Growth in Vitro by the Conjugation of Bmp2 Peptide with Hydroxyapatite on Titanium Alloy. *Colloids Surf., B* doi: 10.1016/j.colsurfb.2013.11.004.
(38) Fan, J.; Park, H.; Lee, M. K.; Bezouglaia, O.; Fartash, A.; Kim, J.; Aghaloo, T.; Lee, M. Adipose Derived Stem Cells and Bmp-2 Delivery in Chitosan-Based 3d Constructs to Enhance Bone Regeneration in a Rat Mandibular Defect Model. *Tissue Eng., Part A* **2014**, DOI: 10.1089/ten.TEA.2013.0523.
(39) Rahman, C. V.; Ben-David, D.; Dhillon, A.; Kuhn, G.; Gould, T. W.; Müller, R.; Rose, F. R.; Shakesheff, K. M.; Livne, E. Controlled Release of BMP-2 from a Sintered Polymer Scaffold Enhances Bone

Repair in a Mouse Calvarial Defect Model. *J. Tissue Eng. Regener. Med.* **2014**, *8*, 59−66.
(40) Del Gaudio, C.; Baiguera, S.; Boieri, M.; Mazzanti, B.; Ribatti, D.; Bianco, A.; Macchiarini, P. Induction of Angiogenesis Using Vegf Releasing Genipin-Crosslinked Electrospun Gelatin Mats. *Biomaterials* **2013**, *34*, 7754−7765.
(41) Rahman, C. V.; Ben-David, D.; Dhillon, A.; Kuhn, G.; Gould, T. W.; Müller, R.; Rose, F. R.; Shakesheff, K. M.; Livne, E. Controlled Release of Bmp-2 from a Sintered Polymer Scaffold Enhances Bone Repair in a Mouse Calvarial Defect Model. *J. Tissue Eng. Regener. Med.* **2014**, *8*, 59−66.
(42) Nijhuis, A. W.; van den Beucken, J. J.; Boerman, O. C.; Jansen, J. A.; Leeuwenburgh, S. C. 1-Step Versus 2-Step Immobilization of Alkaline Phosphatase and Bone Morphogenetic Protein-2 onto Implant Surfaces Using Polydopamine. *Tissue Eng., Part C* **2013**, *19*, 610−619.
(43) Lee, J. H.; Rim, N. G.; Jung, H. S.; Shin, H. Control of Osteogenic Differentiation and Mineralization of Human Mesenchymal Stem Cells on Composite Nanofibers Containing Poly[Lactic-Co-(Glycolic Acid)] and Hydroxyapatite. *Macromol. Biosci.* **2010**, *10*, 173−182.
(44) Shi, Z.; Neoh, K. G.; Kang, E. T.; Poh, C. K.; Wang, W. Surface Functionalization of Titanium with Carboxymethyl Chitosan and Immobilized Bone Morphogenetic Protein-2 for Enhanced Osseointegration. *Biomacromolecules* **2009**, *10*, 1603−1611.
(45) La, W. G.; Kwon, S. H.; Lee, T. J.; Yang, H. S.; Park, J.; Kim, B. S. The Effect of the Delivery Carrier on the Quality of Bone Formed Via Bone Morphogenetic Protein-2. *Artif. Organs* **2012**, *36*, 642−647.
(46) Ben-David, D.; Srouji, S.; Shapira-Schweitzer, K.; Kossover, O.; Ivanir, E.; Kuhn, G.; Muller, R.; Seliktar, D.; Livne, E. Low Dose Bmp-2 Treatment for Bone Repair Using a Pegylated Fibrinogen Hydrogel Matrix. *Biomaterials* **2013**, *34*, 2902−2910.
(47) Bodde, E. W.; Boerman, O. C.; Russel, F. G.; Mikos, A. G.; Spauwen, P. H.; Jansen, J. A. The Kinetic and Biological Activity of Different Loaded Rhbmp-2 Calcium Phosphate Cement Implants in Rats. *J. Biomed. Mater. Res., Part A* **2008**, *87*, 780−791.
(48) Shin, S. Y.; Park, H. N.; Kim, K. H.; Lee, M. H.; Choi, Y. S.; Park, Y. J.; Lee, Y. M.; Ku, Y.; Rhyu, I. C.; Han, S. B.; Lee, S. J.; Chung, C. P. Biological Evaluation of Chitosan Nanofiber Membrane for Guided Bone Regeneration. *J. Periodontol.* **2005**, *76*, 1778−1784.
(49) Dupoirieux, L.; Pourquier, D.; Picot, M. C.; Neves, M. Comparative Study of Three Different Membranes for Guided Bone Regeneration of Rat Cranial Defects. *Int. J. Oral. Max. Surg.* **2001**, *30*, 58−62.
(50) Sirin, Y.; Olgac, V.; Dogru-Abbasoglu, S.; Tapul, L.; Aktas, S.; Soley, S. The Influence of Hyperbaric Oxygen Treatment on the Healing of Experimental Defects Filled with Different Bone Graft Substitutes. *Int. J.Med. Sci.* **2010**, *8*, 114−125.